Supplementary file

Numerical modeling of micro-particle migration in channels

Dongying Wang[1,2,3]*, Qin Qian[1], Anhai Zhong[1], Mingjing Lu[1,2], Zilin Zhang[1]

[1]Petroleum Engineering Technology Research Institute of Shengli Oilfield, Sinopec, Dongying 257000, P. R. China

[2]Postdoctoral Scientific Research Working Station of Shengli Oilfield, Sinopec, Dongying 257000, P. R. China

[3]College of Petroleum of Engineering, China University of Petroleum, Beijing 102249, P. R. China

Emali: t-wangdongying.slyt@sinopec.com (D. Wang); qianqin.slyt@sinopec.com (Q. Qian); zhonganhai.slyt@sinopec.com (A. Zhong); lumingjing001@126.com (M. Lu); zhangzilin.slyt@sinopec.com (Z. Zhang).
ORCID: 0009-0003-4668-9173

This file includes material that complements and expands upon the main article:
Wang, D., Qian, Q., Zhong, A., et al. Numerical modeling of micro-particle migration in channels. Advances in Geo-Energy Research, 2023, 10(2): 117-132.

The link to this file is: https://doi.org/10.46690/ager.2023.11.06

Contents of This File

Introduction

In the Supplementary material, some figures, tables are presented for the purpose of explanation and comparison. They are cited in the main paper file and the supplementary material to assist description of a viewpoint, a model or method and results. Besides, some supporting information for the parameters calculation and detailed description in main text is also presented in this Supplementary Material.

The Figures, Tables and Videos

Table S1 The expressions of variables and coefficients in DEM.

Parameters	Physical meanings	Expression	
		Non-adhesive	Adhesive
a_0	Equilibrium contact region radius	\	$\left(\frac{9\pi\gamma R^2}{E}\right)^{1/3}$
b	Constant	2.283	
E	Effective particle elastic modulus	$(E_iE_j)/\left(E_i(1-\sigma_j^2)+E_j(1-\sigma_i^2)\right)$	
F_C	Critical force	\	$3\pi\gamma R$
F_s^c	Critical sliding force	$\mu_f\|F_n^e\|$	$\mu_f\|F_n^e+2F_C\|$
G	Effective particle shear modulus	$(G_iG_j)/\left(G_i(2-\sigma_j)+G_j(2-\sigma_i)\right)$	
K	Stiffness coefficient	$\frac{4}{3}E\sqrt{R}$	$\frac{4}{3}E\sqrt{R}$
k_n	Elastic stiffness	$\frac{4}{3}E\sqrt{R}\delta_n^{0.5}$	\
k_q	Torsional stiffness	$k_ta^2/2$	
k_r	Rolling stiffness	0	$4F_C(a/a_0)^{1.5}$
k_t	Tangential stiffness coefficient	$8Ga$	
M_t^c	Critical twisting resistance	$3\pi aF_s^c/16$	

M_r^c	Critical rolling resistance	0	$4F_C(a/a_0)^{1.5}\theta_{crit}R$
$\mathbf{n}$	Normal unit vector	$(\mathbf{x}_j-\mathbf{x}_i)/\lvert\mathbf{x}_j-\mathbf{x}_i\rvert$	
R	Effective particle radius	$(r_ir_j)/(r_i+r_j)$	
$\mathbf{t}_r$	Rolling unit vector	$\mathbf{u}_l/\lvert\mathbf{u}_l\rvert$	
$\boldsymbol{t}_s$	Sliding unit vector	$\mathbf{u}_s/\lvert\mathbf{u}_s\rvert$	
$\mathbf{u}_C$	Particle surface velocity at the contact point	$\mathbf{u}_k+r\boldsymbol{\omega}_k\times\mathbf{n}$	
$\mathbf{u}_l$	Rolling velocity	$-R(\boldsymbol{\omega}_i-\boldsymbol{\omega}_j)\times\mathbf{n}-\frac{\mathbf{1}}{\mathbf{2}}\left(\frac{r_j-r_i}{r_j+r_i}\right)\mathbf{u}_s$	
$\mathbf{u}_R$	Relative particle surface velocity at the contact point	$\mathbf{u}_{Ci}-\mathbf{u}_{Cj}$	
$\mathbf{u}_s$	Slip velocity	$\mathbf{u}_R-(\mathbf{u}_R\cdot\mathbf{n})\mathbf{n}$	
w_0	Collision rate before two particles colliding	$\lvert u_i^n-u_j^n\rvert$	
α	Coefficient of friction (function of *e*)	$1.2728-4.2783e+11.087e^2-22.348e^3+27.467e^4-18.022e^5+4.8218e^6$	
δ_C	Critical overlap	\	$\frac{a_0^2}{2(6)^{1/3}R}$
δ_n	Normal overlap	$r_i+r_j-\lvert\mathbf{x}_i-\mathbf{x}_j\rvert$	
η_n	Normal friction coefficient	$\alpha(\mathrm{m}k_n)^{1/2}$	
η_q	Torsional friction coefficients	$\eta_t a^2/2$	
η_r	Rolling friction coefficient	$\mu_r\lvert F_n^e\rvert$	
η_t	Tangential dissipation coefficient	η_n	
μ_r	Rolling coefficient	$(1-e)/\left(bw_0^{1/5}(K/m)^{2/5}\right)$	
ξ_q	Twisting displacement	$\int_{t_0}^{t}\omega_{t(\vartheta)}\,\mathrm{d}\vartheta$	

ξ_r	Rolling displacement	$\int_{t_0}^{t} \mathbf{u}_{l(\vartheta)} \cdot \mathbf{t}_r \, \mathrm{d}\vartheta$
ξ_t	Sliding displacement	$\int_{t_0}^{t} \mathbf{u}_{R(\vartheta)} \cdot \mathbf{t}_s \, \mathrm{d}\vartheta$
ω_t	Relative twisting rate	$(\boldsymbol{\omega}_i - \boldsymbol{\omega}_j) \cdot \mathbf{n}$

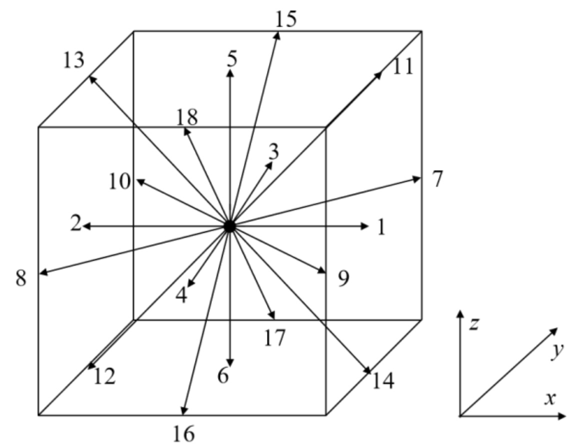

Fig. S1. A lattice node of the D3Q19 model.

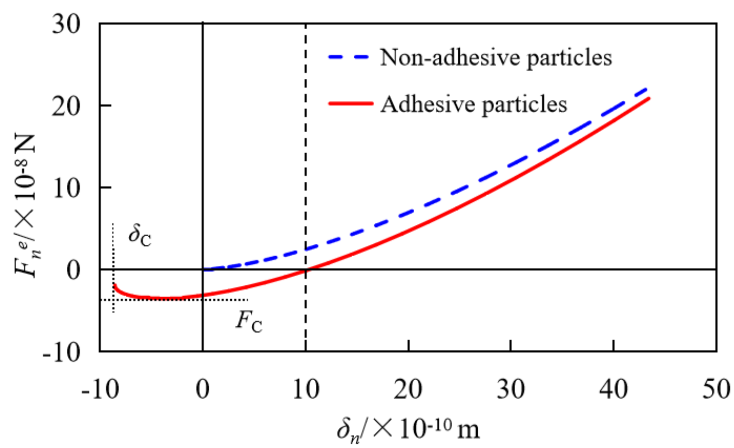

Fig. S2. Variation in the normal elastic force with the overlap of normal particles.

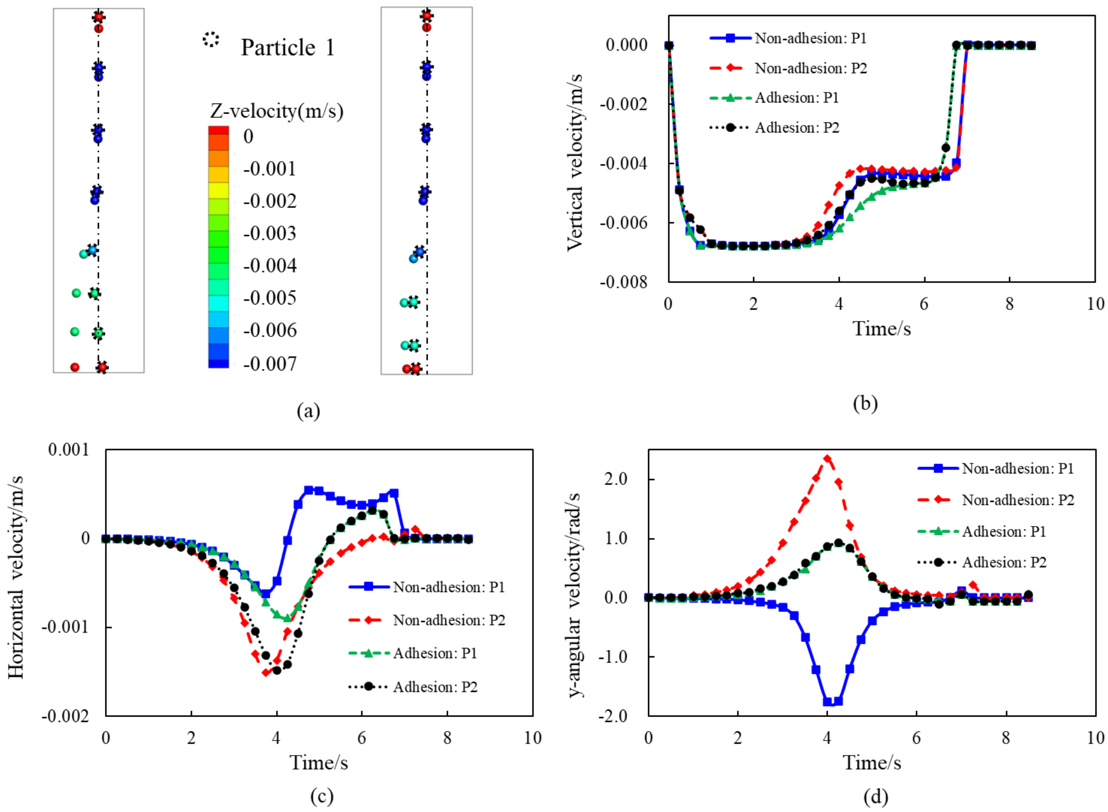

Fig. S3. Trajectories and velocities of particles: (a) Trajectories, (b) Vertical velocity, (c) Horizontal velocity and (d) y-angular velocity.

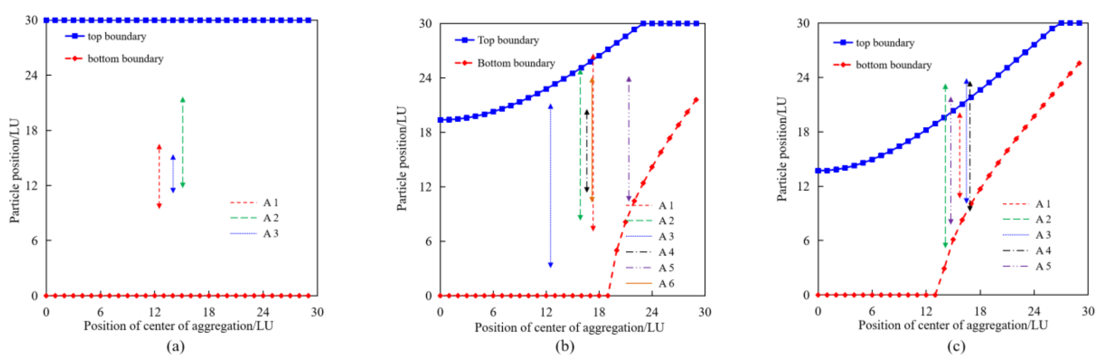

Fig. S4. The stable aggregation distribution map for different Re: (a) Re=6.75, (b) Re=33.75 and (c) Re=67.5.

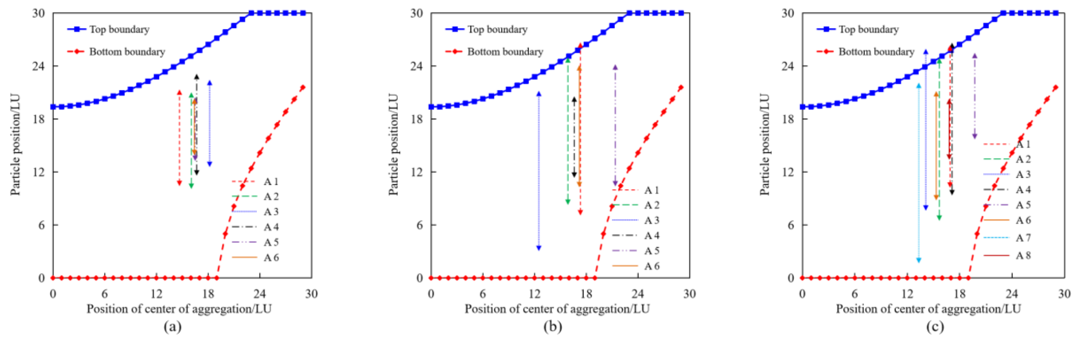

Fig. S5. The stable aggregation distribution map for different particle concentration: (a) C_p=0.5%, (b) C_p=1.0% and (c) C_p=1.5%.

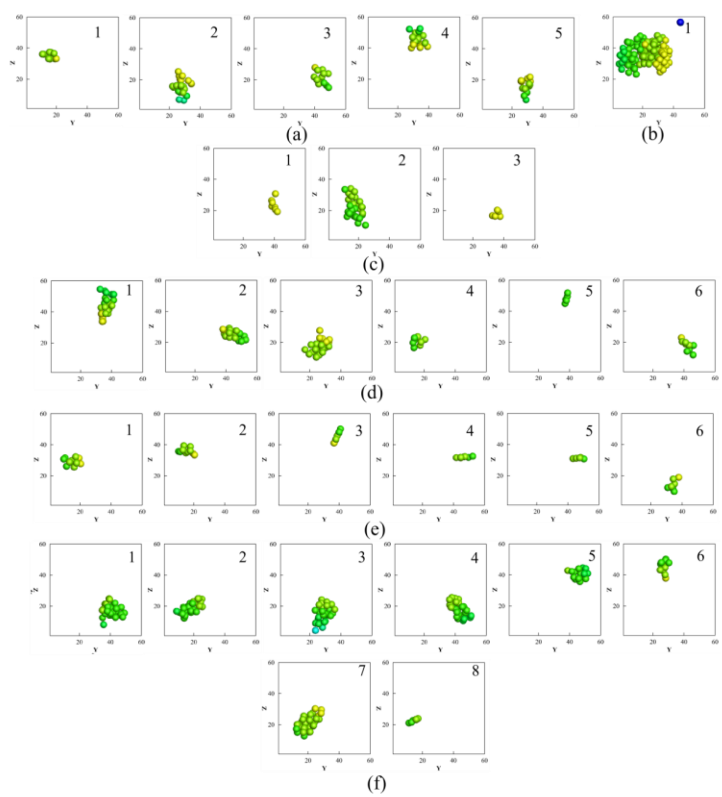

Fig. S6. The lateral position and geometry of each agglomerate under different parameters: (a) Re=67.5, γ=3 mJ/m^2, C_p=1%; (b) Re=67.5, γ=30 mJ/m^2, C_p=1%; (c) Re=6.75, γ=3 mJ/m^2, C_p=1%; (d) Re=33.75, γ=3 mJ/m^2, C_p=1%; (e) Re=33.75, γ=3 mJ/m^2, C_p=0.5% and (f) Re=33.75, γ=3 mJ/m^2, C_p=1.5%.

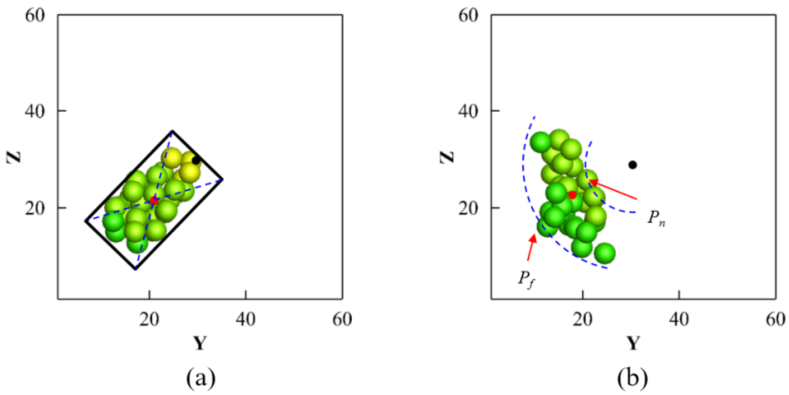

Fig. S7. The determination of positions of agglomerate and member particles: (a) The determination of the agglomerate center and (b) The search of far end particles.

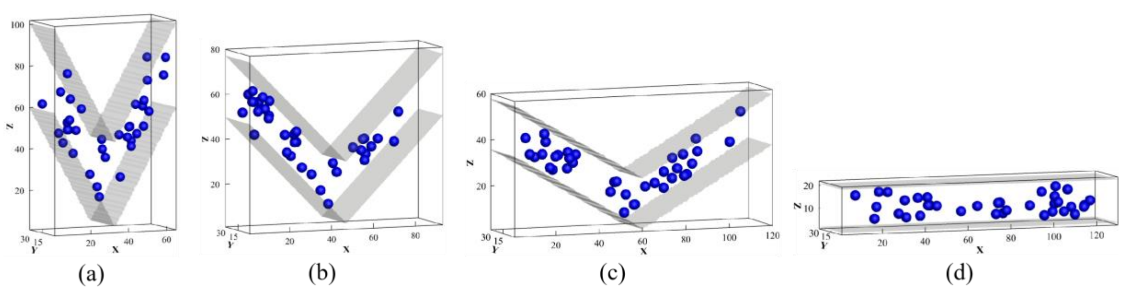

Fig. S8. Geometry of the curved channel and the initial distribution of particles: (a) α=60˚, (b) α=90˚, (c) α=120˚ and (d) α=180˚.

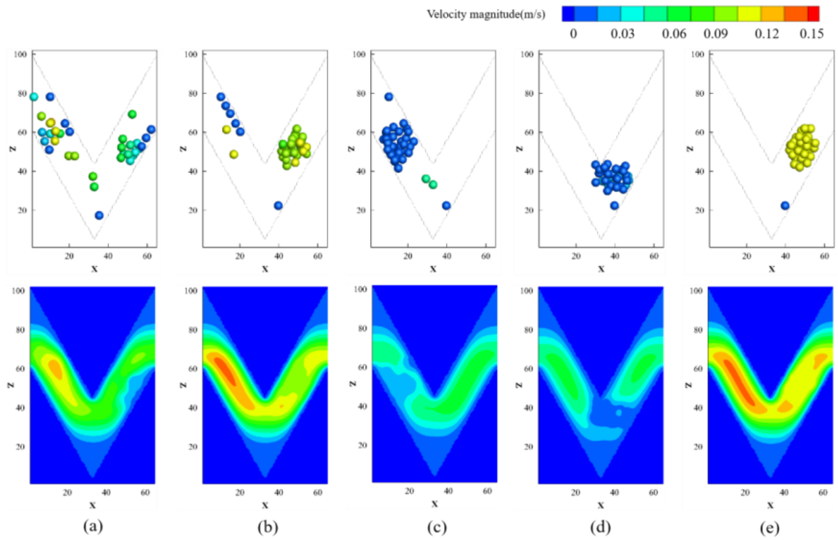

Fig. S9. The evolution of particles distribution in the channel with α=60˚ and the corresponding flow filed.

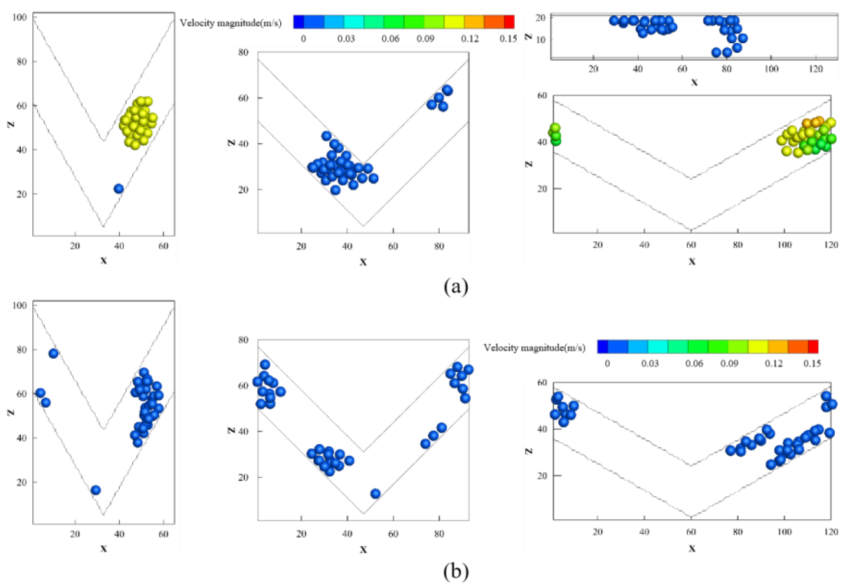

Fig. S10. Final distribution of particles in channels: (a) R_F=0.101 and (b) R_F=0.064.

The link to the **Videos** of particles migration in curved channel: https://pan.baidu.com/s/1rNBRCe9oKoU5weEEmIQcpA, Code: tor8.